

# Atom probe Tomography of fast-diffusing impurities and the effect of gettering in multicrystalline silicon

Cite as: AIP Conference Proceedings **1999**, 130019 (2018); <https://doi.org/10.1063/1.5049338>

Published Online: 10 August 2018

David Tweddle, Eleanor C. Shaw, James O. Douglas, Ruy S. Bonilla, Michael P. Moody, Phillip Hamer, and Peter R. Wilshaw



View Online



Export Citation

## ARTICLES YOU MAY BE INTERESTED IN

[Role of hydrogen: Formation and passivation of meta-stable defects due to hydrogen in silicon](#)

AIP Conference Proceedings **1999**, 130010 (2018); <https://doi.org/10.1063/1.5049329>

[Investigation of temperature and illumination dependencies of carrier-induced degradation in p-type multi-crystalline silicon](#)

AIP Conference Proceedings **1999**, 130014 (2018); <https://doi.org/10.1063/1.5049333>

[Modelling of hydrogen transport in silicon solar cell structures under equilibrium conditions](#)

Journal of Applied Physics **123**, 043108 (2018); <https://doi.org/10.1063/1.5016854>

## Lock-in Amplifiers up to 600 MHz

starting at

\$6,210



 Zurich Instruments

Watch the Video



# Atom Probe Tomography of Fast-Diffusing Impurities and the Effect of Gettering in Multicrystalline Silicon

David Tweddle<sup>1, a)</sup>, Eleanor C. Shaw<sup>1</sup>, James O. Douglas<sup>1</sup>, Ruy S. Bonilla<sup>1</sup>,  
Michael P. Moody<sup>1</sup>, Phillip Hamer<sup>1</sup> and Peter R. Wilshaw<sup>1</sup>

<sup>1</sup> *University of Oxford, Department of Materials, 16 Parks Road, Oxford, OX1 3PH, UK*

<sup>a)</sup> Corresponding author: david.tweddle@materials.ox.ac.uk

**Abstract.** This article demonstrates an approach for multiscale characterisation of individual defects, such as grain boundaries, in multicrystalline silicon. The analysis techniques range from macroscale characterisation of average bulk lifetime, through photoluminescence to resolve spatial recombination, and finally to nanoscale analysis of the crystallographic characteristics and impurity decoration of the grain boundary using Transmission Kikuchi Diffraction and Atom Probe Tomography. This method can be used to characterise defects and their response to processing, such as gettering and hydrogen passivation. In this paper it is applied to the test case of Saw Damage Gettering on Red Zone High Performance Multicrystalline Silicon. In both as-cast and gettered samples, copper and chromium were observed at a recombination active, random angle grain boundary. After gettering the copper excess was found to decrease. In contrast, the slower diffusing chromium was found to increase, potentially indicating internal gettering. At a recombination inactive  $\Sigma 3$  grain boundary only oxygen was observed at the boundary before gettering, with no transition metals detected.

## INTRODUCTION

Defect engineering, defined as reducing the effect of crystallographic defects and impurities on the electrical properties, is a major research focus in multicrystalline silicon solar cells. Together gettering and hydrogenation have become industry standard techniques for achieving high bulk lifetimes and hence higher efficiency solar cells. Gettering involves the redistribution of impurities from both the bulk and crystallographic defects to a less active region, during a high temperature firing process. In contrast, hydrogenation reduces the electrical activity of such defects, via chemical bonding to impurities. Since both techniques fundamentally interact with bulk crystallographic defects, such as grain boundaries and dislocations, further understanding is required for future optimisation.

With the recent development of High Performance Multicrystalline (HPMC) silicon, which utilises smaller grains, grain boundaries and how they interact with dislocations and impurities has become of increased importance [1]–[3]. The orientation of a grain boundary has been strongly linked to its recombination activity, with small angle grain boundaries i.e., grain boundaries with a misorientation angle below 15°, are found to be the most detrimental to the electrical performance [4]. Although there a number of techniques that are able to characterise the electrical activity of such grain boundaries, accurately analysing both the composition and structure of the defects present has proved difficult.

This paper presents the use of a multiscale technique approach, characterising HPMC silicon wafers on both the macro and nano –scales and then finally on the near atomic-scale using Atom Probe Tomography (APT). APT, which utilises time-of-flight mass spectrometry with a position sensitive detector, is uniquely placed to resolve the 3D location of individual atoms segregated to the grain boundary, as well as their identity and composition. Depth and lateral spatial resolutions of  $\sim 0.2$  and  $\sim 0.4$  nm respectively are achievable [5], in combination with local impurity detection limits down to ppm levels, depending on the spatial segregation of impurities, potential mass spectra overlaps and the signal to background ratio [6]. This technique therefore, in association with crystallographic information from Transmission Kikuchi Diffraction (TKD), allows for a detailed characterisation of an individual grain boundary.

This approach was applied to samples before and after Saw Damage Gettering (SDG). This technique utilises the surface damage layer caused by diamond wire sawing of wafers, in combination with a specific thermal treatment to reduce metallic impurity concentrations [7], via preferential precipitation of impurities in the saw damaged region. This gettering process was selected as an ideal model for measuring the efficacy of our multiscale characterisation, due to the simplicity of the technique. SDG relies purely on heat and preferential precipitation and does not result in the same injection of interstitials seen in Phosphorus Diffusion Gettering (PDG) [8].

## EXPERIMENTAL METHODS

The materials used in this study are sister wafers taken from the bottom of the ingot or Red Zone of a high performance (HPRZ) multicrystalline ingot. The p-type wafers have an initial thickness of 180  $\mu\text{m}$  ( $\pm 5 \mu\text{m}$ ), a resistivity of 0.3  $\Omega\cdot\text{cm}$  ( $\pm 0.05 \Omega\cdot\text{cm}$ ) and a corresponding boron doping concentration of  $6 \times 10^{16} \text{ cm}^{-3}$ . This material was chosen due to the higher levels of impurities, in order to improve impurity detection in APT. SDG was applied to a number of silicon carbide slurry wire sawn wafers with initial start temperatures of 850 °C and 900 °C for 10 minutes followed by an exponential cool to 500 °C over 50 minutes in a tube furnace with a nitrogen ambient [7]. To investigate the efficacy of the SDG process, the same thermal treatment was applied to sister wafers where the saw damage has been chemically removed using an acidic etch (No-SDG). Additionally some wafers were removed early during the exponential cool from 900 °C at temperatures between 500-800 °C. The saw damaged layer was then removed using a chemical etch consisting of hydrofluoric acid, nitric acid and acetic acid (HNA), followed by the deposition of a PECVD SiNx:H layer using an Oxford Instruments Plasmalab 80 plus. The wafers were then characterised using photoconductance measurements (Sinton WCP-120) analysed with the generalised method [9]. The interstitial iron concentration was then determined using photoconductance measurements after illumination and dark storage following the method of MacDonald *et al.* [10]. The spatial distribution of recombination centres of two selected sister wafers, one of which had the 900 °C to 500 °C SDG process and the other As-Cast were then imaged using uncalibrated photoluminescence (BT Imaging LIS-L1) [11]. The nitride layer was then chemically removed during sample etching using a further HNA etch prior to APT analysis.

Grain boundary containing APT needles were lifted out using focused ion beam methods, as described in [12]. This allows for correlative transmission electron microscopy (TEM), TKD and APT with the grain boundary running along the tip direction, enabling a comparatively large length of grain boundary to be studied. TKD of the two grain boundaries was analysed using a Zeiss Crossbeam FIB/SEM at an acceleration voltage of 30 kV and beam current of 2 nA. APT was performed by a Cameca LEAP 5000 XR at a temperature of 50K, pulse frequency of 200 kHz, laser energy of 50 pJ with a UV wavelength of 355 nm and detection rate of 2.0 %.

## MACROSCOPIC ANALYSIS

The application of SDG on p-type HPRZ greatly improved the minority carrier lifetime, as shown in Figure 1a. When comparing the lifetime of the SDG groups to the As-Cast group, or the No-SDG group (heat treatment applied but without saw damage), it is shown that the combination of saw-damage and the thermal treatment is necessary to provide improvement in lifetime. The interstitial iron concentration, which is readily observed via lifetime spectroscopy, was also reduced for the SDG groups.

Although using minority carrier lifetime spectroscopy to determine which impurities are the dominant sources of recombination is not possible, the results presented in Figure 1c allow some conclusions to be drawn. When samples were removed above 700 °C the lifetime after gettering was reduced, indicating that the lifetime limiting impurities are highly mobile in silicon at temperatures below 700 °C. This suggests that faster diffusing elements, such as Cu and Ni are important for recombination, in contrast to slower diffusing elements such as Fe and Cr [13].

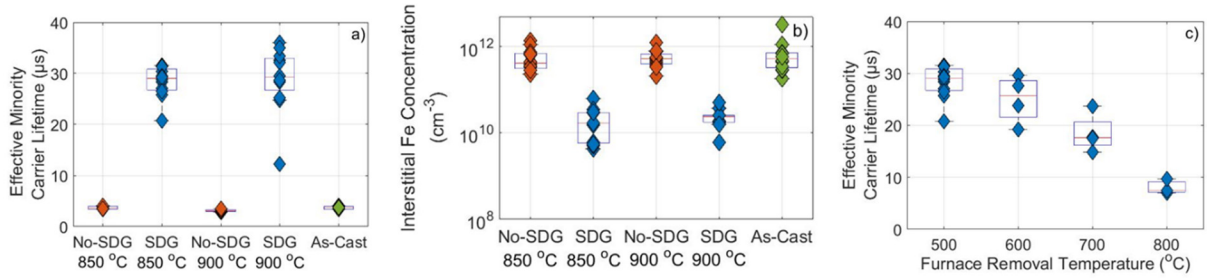


**FIGURE 1.** a) Lifetime for different SDG processing routes, b) Interstitial Fe concentration for different SDG processing routes, c) Lifetime for specimens removed at a range of temperatures compared to the standard 500 °C.

In order to investigate the distribution of lifetime before and after gettering, photoluminescence was used, as shown in Figure 2. Prior to gettering, the lifetime of both the bulk and at grain boundaries is extremely low. Following SDG, intragrain lifetimes are significantly improved. However, most grain boundaries still remain significantly recombination active, albeit some grain boundaries are much more reactive than others. The two grain boundaries of varying recombination activities (GB 1 and GB 2), which were selected for further analysis are marked in Figure 2.

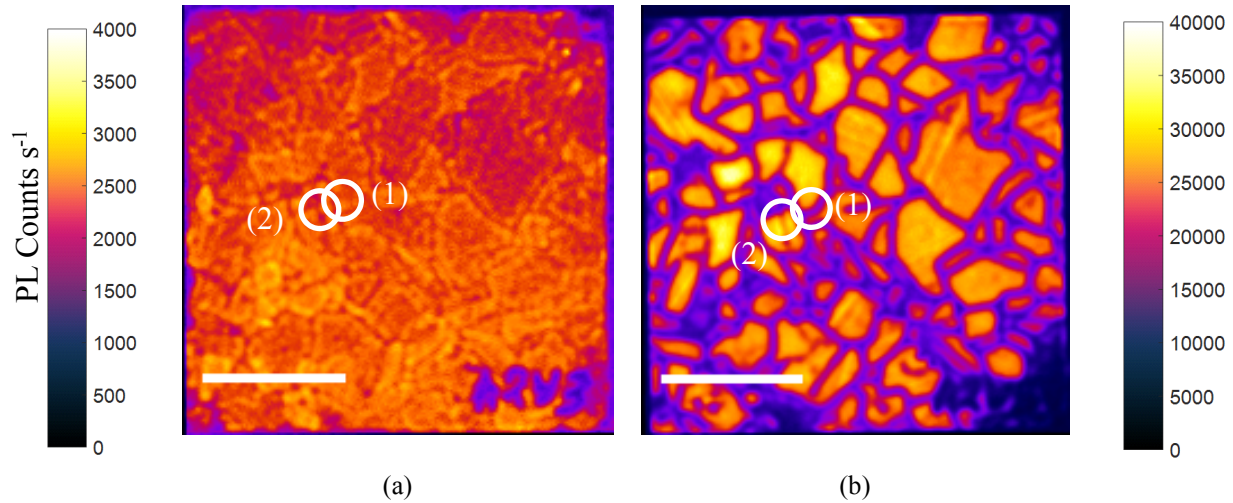
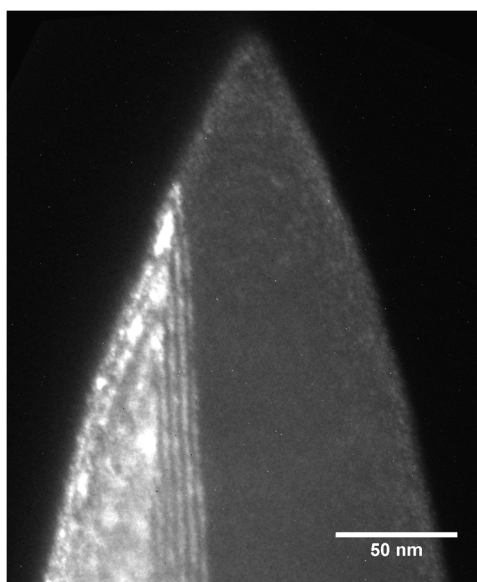


**FIGURE 2.** Photoluminescence images of HPRZ sister wafers before (a) and after (b) saw damage gettering. The grain boundaries selected for further analysis are marked. Scale bars 10 mm.

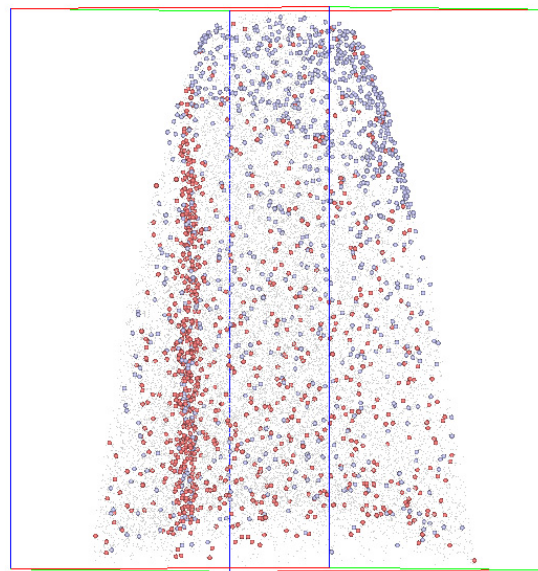
## NANOSCALE ANALYSIS

Following macroscale analysis of both lifetime and composition, two grain boundaries were selected for analysis with varying recombination activities. As seen in Figure 2, the recombination activity of GB 1 is much greater after SDG compared to that of GB 2. Using TKD, this boundary was confirmed as a large random angled grain boundary, with a misorientation of 45°. In order to investigate the impurity distribution and concentration at these grain boundaries, atom probe samples containing grain boundaries from gettered and ungettered sister wafers were fabricated.

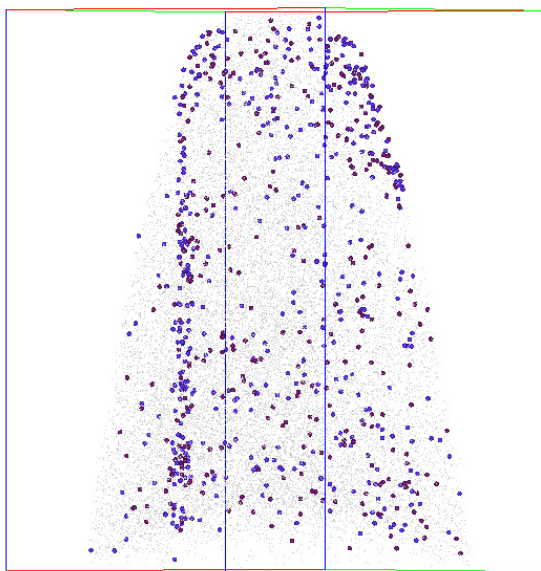




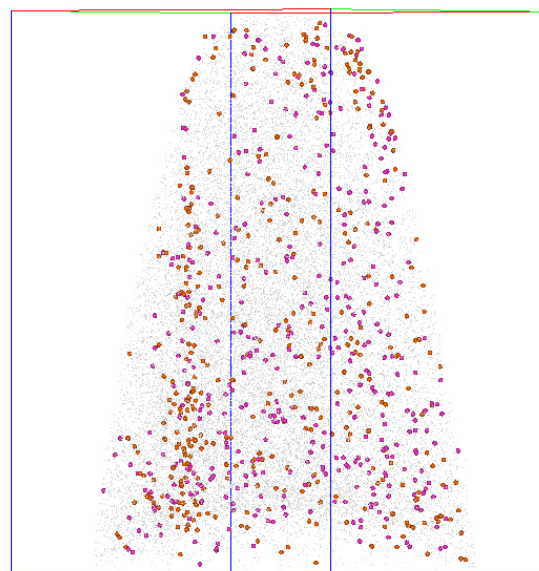
(a)



(b)



(c)



(d)

**FIGURE 3.** Dark field transmission electron micrograph (a) and subsequent atom probe 3D reconstruction of GB 1 in the pre-gettered wafer. (b)  $\text{SiO}$  and  $\text{SiC}$ , (c)  $\text{Si}_2\text{N}$  and  $\text{SiN}$ , (d)  $\text{Cr}$  and  $\text{Cu}$ . The grain boundary is shown enriched in oxygen, carbon, nitrogen, chromium and copper. A small fraction of silicon atoms (grey) are shown for reference. Scale bars 20 nm for b, c, d.

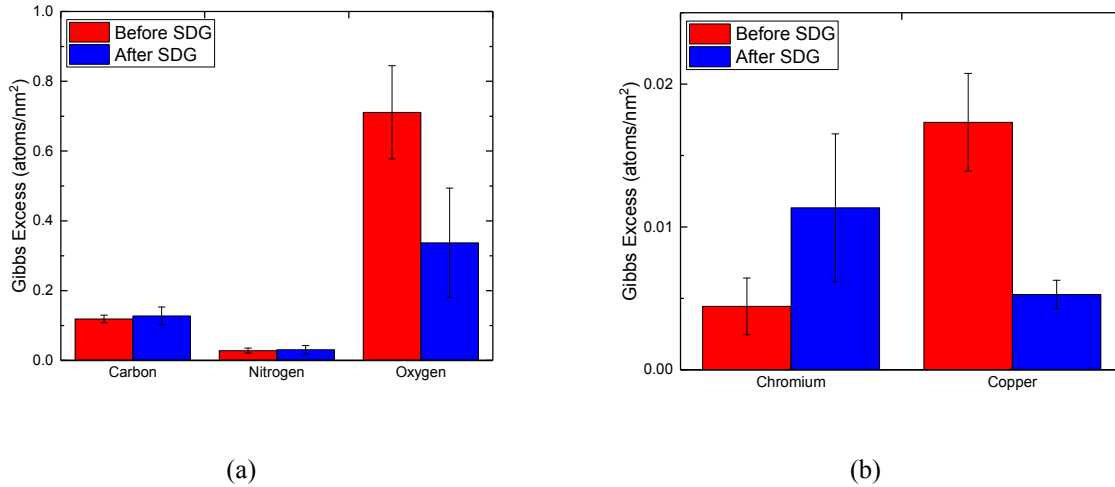
The sample shown in Figure 3a was analysed by APT directly following TEM, in order to determine the composition at the grain boundary. The grain boundaries are marked by the presence of the transition metals such as Cr and Cu, in addition to the lighter elements C, O and N, as shown in Figure 3. The transition metals decorating the

grain boundary do not exhibit any evidence of clustering or the formation of precipitates, but appear to be distributed near homogenously throughout the boundary. To quantify the impurity excess at the grain boundary of these different elements before and after gettering, the Gibbsian interfacial excess for both C, N, O, Cr and Cu was calculated using Equation 1, as described in [14].

$$\Gamma = \frac{N(c_i - c_{i(\alpha)})}{A\eta} \quad (1)$$

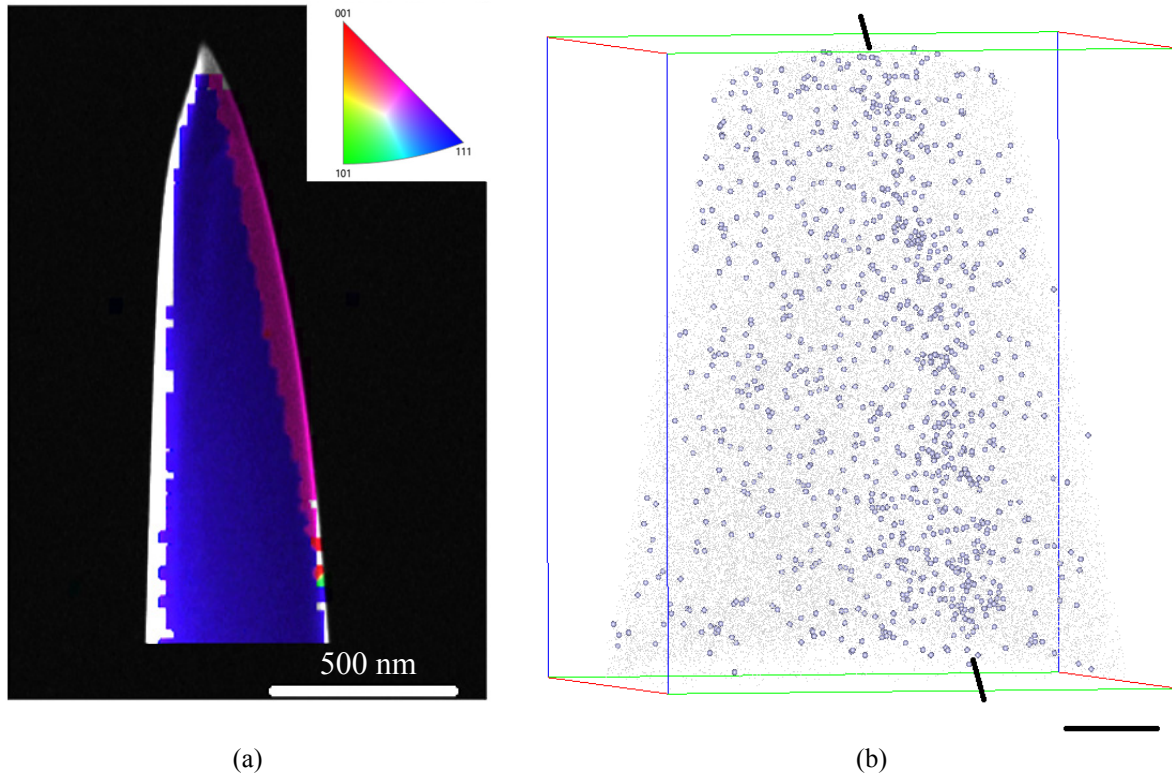
Where  $\Gamma$  is the interfacial excess in atoms/nm<sup>2</sup>, N is the number of atoms in the volume of the grain boundary containing region of interest,  $c_i$  and  $c_{i(\alpha)}$  are the concentrations of impurities at the grain boundary and bulk respectively,  $\eta$  is the detection efficiency (52% on LEAP 5000 XR) and A is the cross sectional area of the volume analysed. A number of different volumes were sampled in the bulk and at the grain boundaries, with the average bulk and grain boundary concentrations calculated.

Figure 4 shows the excess of the elements which are shown to segregate to grain boundaries in Figure 3. For GB 1, which has a high recombination activity before and after SDG, significant concentrations of copper are observed at the grain boundary. However, the level of copper is seen to decrease by a factor of a half after gettering, indicating SDG is successful at removing this element. This is also true for oxygen, which reduces in concentration significantly following SDG. In contrast, slower diffusing Cr actually increases in concentration following SDG



**FIGURE 4.** Gibbsian excess values for GB 1 before and after SDG, for a) C, N, O and b) Cr, Cu.

The second grain boundary analysed showed very little recombination activity in the photoluminescence images. It was therefore expected that less decoration would be visible on this grain boundary, most likely due to weaker segregation. Figure 5 presents TKD and atom probe images of this grain boundary with no gettering. From the TKD Y inverse pole figure map, it was possible to determine the boundary as a  $\Sigma 3$  twin boundary and also to ensure the grain boundary is in the APT sample prior to analysis. This boundary has been widely reported [15]–[17] to be less recombination active and to be a weak gettering site for impurities. This is borne out by the atom probe results, which observed no significant decoration of the grain boundary by metallic impurities, carbon or nitrogen. Indeed, the only means of clearly observing the grain boundary in the atom probe reconstruction was through elevated levels of oxygen. For the sample after SDG, the grain boundary was extremely difficult to detect in APT, presumably due to a reduction in oxygen concentration similar to that observed for GB 1. While this makes it difficult to be certain where the grain boundary was located in the atom probe needle, there was no evidence of any gettering of copper or chromium to GB 2 in the SDG sample.



**FIGURE 5.** (a) TKD image of a twin grain boundary, with colours showing the Y inverse pole figure. (b) Atom probe 3D reconstruction of GB 2 in the pre-gettered wafer showing a slight enrichment in SiO at the boundary. A small fraction of silicon atoms (grey) are shown for reference. Scale bar 20 nm for b.

## DISCUSSION

Bulk lifetime measurements, shown in Figure 1a, clearly demonstrate the effectiveness of SDG as a gettering technique. However, this improvement is largely in the intra-grain regions, leaving the grain boundaries as the primary sources of recombination in the getterted wafer. The recombination activity of grain boundaries in multicrystalline silicon is known to depend strongly upon the orientation of the boundary and decoration with metallic impurities. In light of previous results in the literature [15]–[17], it is unsurprising that the more recombination active grain boundary (GB 1) was determined to be random angle, while the almost inactive grain boundary was a  $\Sigma 3$  twin.

It is also expected that GB 1 would show high concentrations of a large number of metallic impurities, only Cu and Cr were observed at the grain boundary. Surprisingly no Fe or Ni was seen, although they are known impurities in multicrystalline silicon, often seen in large quantities [18]. The lack of detected Fe at grain boundaries may be caused the presence of large intragranular Fe clusters, as seen by Istratov [19], which are termed efficient gettering sites and can in fact improve diffusion lengths. In contrast, the distribution of Cu and Cr along the boundary, was found to be homogenous with no direct evidence of clustering or precipitation. This is in contrast to results by Buonassisi [18], who observed a number of nanoprecipitates elongated along the grain boundary direction. Although it is not possible to exclude the presence of such precipitates with the small sample volumes, it is interesting to note that a homogenous distribution is observed. This is thought to have a much greater effect on the recombination activity of the defect, compared to a small number of large, widely distributed precipitates [20].

Since GB 2 was found to be a  $\Sigma 3$  grain boundary and is almost electrically inactive, it was expected to have very low levels of metallic impurities. This is as a result of coherent  $\Sigma 3$  grain boundaries having lower levels of strain and much fewer nucleation sites for impurities [1]. In this study, prior to gettering, the grain boundary is only observed by a small increase in oxygen content at the grain boundary. This result supports conclusions drawn by Ohno [21] who, using APT, observed no transition metal impurities located at a  $\Sigma 3$  grain boundary. Following SDG, which is found to

reduce oxygen concentrations at grain boundaries (Figure 4a), determining whether a grain boundary is present becomes difficult, albeit no evidence of transition metal impurities were present.

The main drawback of the TKD and APT analysis process is the time required to prepare and characterise a sample. This means that it is prohibitively difficult to analyse comparatively large sections of a grain boundary. While the technique used in this work, described in detail in [12], allows for larger areas of grain boundary to be analysed in a single sample, it is still not possible to establish statistical certainty as to the decoration of the entire grain boundary. Nonetheless, in combination with microscopic recombination characterisation using photoconductance and photoluminescence, it is possible to draw some tentative conclusions as to the critical impurities responsible for recombination in HPRZ samples before and after SDG.

Copper is a known fast diffuser in silicon [13], and is present in large quantities in red zone material. Although recombination as an interstitial atom is known to be weak, copper is found to decorate defects [22] and increase their recombination. Since Cu is highly soluble in silicon, a longer cool is likely important for effective gettering. Although SDG has significantly reduced the quantities of copper at the grain boundary, its presence after PDG is still likely to be responsible for at least part of the recombination activity.

Chromium is also seen in reasonable quantities at GB 1 before and after gettering. The results suggest that the gettering process does not reduce Cr at the grain boundaries, although it is not clear whether this is due to Cr not being released from the grain boundaries or segregating to the boundaries during gettering. Chromium is a known strong recombination centre [23] however, due to its low diffusivity, it is unlikely to be the limiting factor in intra-grain lifetimes prior to gettering. It is however likely that grain boundary recombination activity after gettering is still affected by Cr.

Nickel has a high solubility, diffusivity and recombination activity in silicon [13], and has been previously seen to reside at grain boundaries [24], making it a prime suspect for causing strong recombination activity. However no Ni was detected at GB 1, therefore making it unlikely that Ni plays a role in grain boundary recombination. Since Ni behaves in a similar manner to Cu, it is expected that the bulk concentration of Ni is also fairly low.

The detection of Fe using APT is challenging, due to the overlap between  $^{56}\text{Fe}^{2+}$  and  $^{28}\text{Si}^+$ , both at 28 Da, in addition to the presence of  $^{28}\text{Si}_2^+$  multiples which overlap with  $^{56}\text{Fe}^+$ . It is therefore necessary to use the minor isotope of Fe at 54 Da for detection. For GB 1, both before and after gettering, no evidence of Fe at the grain boundary was found. This suggests that Fe does not play a significant role in grain boundary recombination. However Fe is a known impurity, present in high concentrations in red zone material (Figure 1b), suggesting that Fe is located in intra-grain regions, potentially as large Fe clusters discussed above.

The reduction in copper after SDG for GB 1 and the lifetime results (Figure 1c), in which a slow cool is required for high lifetimes, supports the hypothesis that copper is a primary element responsible for the increased lifetimes observed. As a result of industry time and cost pressures, phosphorus diffusion gettering (PDG) does not usually involve any form of slow cool [ref]. It is therefore possible that the strong activation of grain boundaries after PDG, found by Sio [3], is due to insufficient driving force for copper to be efficiently getterred to the phosphorus region.

## CONCLUSIONS

This paper attempts to perform a multiscale characterisation of grain boundaries at different stages of processing. The processing technique chosen to demonstrate this method is saw damage gettering, selected for its simplicity. Correlative TKD, TEM and APT was shown to be effective at characterising grain boundaries in sister wafers, allowing for crystallographic and compositional analysis.

The random angle grain boundary (GB 1) was found to contain elevated levels of Cu and Cr both before and after SDG, which are thought to be the cause of the high recombination activity. These impurities are found to be homogeneously distributed along the grain boundary, with no evidence of clustering or precipitation. The slow cooling process involved in SDG is thought to be cause of the efficient removal of Cu from the grain boundary, with Cu thought to be the cause of the lower lifetimes when higher temperature quenching is performed. Slower diffusing Cr still remains at the grain boundary after gettering, although it is not known whether this is due to internal grain boundary gettering from the bulk or binding of Cr already present.

The  $\Sigma 3$   $\langle 111 \rangle$  grain boundary (GB 2) had a much lower recombination activity than GB 1, likely due to the lack of metallic impurities observed at the boundary. Prior to gettering, the boundary was observed in APT via increased levels of oxygen, which are known to getter via SDG. It is therefore difficult to ascertain whether the grain boundary was analysed from the getterred wafer, although no metallic impurities were observed.



## ACKNOWLEDGEMENTS

The authors would like to acknowledge financial support from Lincoln College, Oxford and also from the UK government through the EPSRC (Supersilicon grant, EP/M024911/1). In addition, the Zeiss Crossbeam FIB/SEM used in this work was supported by EPSRC through the Strategic Equipment Fund, grant EP/N010868/1.

## REFERENCES

- [1] K. Adamczyk *et al.*, “Recombination activity of grain boundaries in high-performance multicrystalline Si during solar cell processing,” *J. Appl. Phys.*, vol. 12, no. 5, p. 055705, 2018.
- [2] A. Autruffe *et al.*, “High performance multicrystalline silicon: Grain structure and iron precipitation,” *J. Appl. Phys.*, vol. 122, 135103, 2017.
- [3] H. C. Sio *et al.*, “Recombination sources in p-type high performance multicrystalline silicon,” *Jpn. J. Appl. Phys.*, vol. 56, 08MB16, Aug. 2017.
- [4] J. Chen *et al.*, “Electron-beam-induced current study of small-angle grain boundaries in multicrystalline silicon,” *Scr. Mater.*, vol. 52, no. 12, pp. 1211–1215, Jun. 2005.
- [5] Y. Shimizu *et al.*, “Atom probe microscopy of three-dimensional distribution of silicon isotopes in Si28/ Si30 isotope superlattices with sub-nanometer spatial resolution,” *J. Appl. Phys.*, vol. 106, p. 076102, 2009.
- [6] B. Gault, M. P. Moody, J. M. Cairney, and S. P. Ringer, *Atom Probe Microscopy*. Springer, 2012.
- [7] E. C. Shaw, P. Hamer, K. A. Collett, G. Bourett-Sicotte, R. S. Bonilla, and P. R. Wilshaw, “Saw Damage Gettering for industrially relevant mc-Si feedstock,” *Phys. Status Solidi Appl. Mater. Sci.*, vol. 214, 170037, no. 7, Jul. 2017.
- [8] M. L. Polignano, G. F. Cerofolini, H. Bender, and C. Claeys, “Gettering mechanisms in silicon,” *J. Appl. Phys.*, vol. 62, no. 2, pp. 869–876, 1988.
- [9] H. Nagel, C. Berge, and A. G. Aberle, “Generalized analysis of quasi-steady-state and quasi-transient measurements of carrier lifetimes in semiconductors,” *J. Appl. Phys.*, vol. 86, no. 11, pp. 6218–6221, 1999.
- [10] D. Macdonald, L. J. Geerligs, and A. Azzizi, “Iron detection in crystalline silicon by carrier lifetime measurements for arbitrary injection and doping,” *J. Appl. Phys.*, vol. 95, no. 3, pp. 1021–1028, 2004.
- [11] T. Trupke, R. Bardos, M. Schubert, and W. Warta, “Photoluminescence imaging of silicon wafers,” *Appl. Phys. Lett.*, vol. 89, no. 4, pp. 044107–044107, 2006.
- [12] C. Lotharukpong *et al.*, “Specimen preparation methods for elemental characterisation of grain boundaries and isolated dislocations in multicrystalline silicon using atom probe tomography,” *Mater. Charact.*, vol. 131, pp. 472–479, 2017.
- [13] E. R. Weber, “Transition metals in silicon,” *Appl. Phys. A Mater. Sci. Process.*, vol. 30, no. 1, pp. 1–22, 1983.
- [14] M. K. Miller and G. D. W. Smith, “Atom probe analysis of interfacial segregation,” *Appl. Surf. Sci.*, vol. 87–88, no. 94, pp. 243–250, 1995.
- [15] M. S. Wiig, K. Adamczyk, H. Haug, K. E. Ekstrøm, and R. Søndenå, “The Effect of Phosphorus Diffusion Gettering on Recombination at Grain Boundaries in HPMC-Silicon Wafers,” *Energy Procedia*, vol. 92, no. 1876, pp. 886–895, 2016.
- [16] Y. M. Yang, A. Yu, B. Hsu, W. C. Hsu, A. Yang, and C. W. Lan, “Development of high-performance multicrystalline silicon for photovoltaic industry,” *Prog. Photovoltaics Res. Appl.*, vol. 23, pp. 340–351, 2015.
- [17] J. Chen, D. Yang, Z. Xi, and T. Sekiguchi, “Recombination activity of sigma 3 boundaries in boron-doped multicrystalline silicon: Influence of iron contamination,” *J. Appl. Phys.*, vol. 97, no. 3, p. 033701, 2005.
- [18] T. Buonassisi *et al.*, “Chemical natures and distributions of metal impurities in multicrystalline silicon materials,” *Prog. Photovoltaics Res. Appl.*, vol. 14, no. 6, pp. 512–531, 2006.
- [19] A. A. Istratov *et al.*, “Metal content of multicrystalline silicon for solar cells and its impact on minority carrier diffusion length,” *J. Appl. Phys.*, vol. 94, no. 10, pp. 6552–6559, 2003.
- [20] T. Buonassisi *et al.*, “Synchrotron-based investigations of the nature and impact of iron contamination in multicrystalline silicon solar cells,” *J. Appl. Phys.*, vol. 97, no. 7, p. 074901, 2005.
- [21] Y. Ohno *et al.*, “Three-dimensional evaluation of gettering ability of sigma 3 {111} grain boundaries in silicon by atom probe tomography combined with transmission electron microscopy,” *Appl. Phys. Lett.*, vol. 103, no. 10, pp. 12–16, 2013.
- [22] Y. Ohno *et al.*, “Nanosopic mechanism of Cu precipitation at small-angle tilt boundaries in Si,” *Phys. Rev. B - Condens. Matter Mater. Phys.*, vol. 91, p. 235315, 2015.

- [23] G. Coletti, “Sensitivity of state-of-the-art and high efficiency crystalline silicon solar cells to metal impurities,” *Prog. Photovoltaics Res. Appl.*, vol. 21, pp. 1163–1170, Mar. 2013.
- [24] Y. Ohno *et al.*, “Recombination activity of nickel, copper, and oxygen atoms segregating at grain boundaries in mono-like silicon crystals,” *Appl. Phys. Lett.*, vol. 109, p. 142105, 2016.